IEEE Access
Multidisciplinary | Rapid Review | Open Access Journal

Received September 20, 2018, accepted October 4, 2018, date of publication October 15, 2018, date of current version November 8, 2018.

Digital Object Identifier 10.1109/ACCESS.2018.2876040

Robotics for Seabed Teleoperation: Part-1—Conception and Practical Implementation of a Hybrid Seabed Robot

ROQUE SALTAREN, ALEJANDRO RODRÍGUEZ BARROSO, AND OZ YAKRANGI
Centro de Automática y Robótica CAR UPM-CSIC, Universidad Politécnica de Madrid, 28040 Madrid, Spain

Corresponding author: Roque Saltaren (roquejacinto.saltaren@upm.es)

This work was supported in part by the Spanish Government Projects under Grant DPI2009-08778, Grant DPI2014-57220-C2-1-P, and Grant DPI2013-49527-EXP, in part by the Universidad Politécnica de Madrid Project under Grant AL14-PID-15, and in part by the RoboCity2030-III-CM Project (Robótica aplicada a la mejora de la calidad de vida de los ciudadanos. Fase III) under Grant S2013/MIT-2748, in part by the Programas de Actividades I + D en la Comunidad de Madrid, and in part by Structural Funds of the EU.

ABSTRACT Remote exploration and work on the seabed require special-use robots that are adapted to both working on rough surfaces and traveling through an underwater environment. This paper discusses a prototype design for a hybrid robot that moves like a submarine in one configuration and like a humanoid in another. This hybrid design allows the robot to move efficiently on the work surface and execute its functions on that surface with human-like movements. Moreover the robot has hydraulic actuators with 24 degrees of freedom. Furthermore, this paper discusses design choices and preliminary tests related to navigation, transformation from one configuration to another, and a gestural teleoperation control scheme.

INDEX TERMS Aquatic robots, humanoid robots.

I. INTRODUCTION

The underwater robotic technology for navigation, exploration, and manipulation in marine environments has been used since many years. However, underwater robots still face complex problems associated with their autonomy, manipulation, perception, and communication [1]. Another unsolved problem is that underwater robots have still not seen relevant developments concerning their operation on seabeds. Presently, there is a significant need of new technologies for exploration and operation on the seabed. Therefore, underwater robotic technologies will be show a meaningful contribution in this regard in the future. Accordingly, this work deals with the development of a hybrid robot that can work on a seabed as a robot with legs and humanoid kinematics remotely controlled with the bodily movements of a human operator [2].

Researchers consider using servo-hydraulic technologies to demonstrate that through a modular design, it is possible to solve the mechanical and control complexity of a 24 degrees of freedom robot that can work at any depth and move over irregular marine surfaces with slopes and ravines. As a result, an anthropomorphic compact submarine robot was developed. This robot is robust and lightweight; it can be easily controlled through gestures and natural movements of the remote operator.

Due to the complexity of the project, the research is categorized into two parts. The first part presents the conception as well as the development and experimental results. In second part, mathematical modeling and the control of the underwater hybrid robot are presented.

A. DESIGN BASED ON BIOLOGICAL INSPIRATION

In remote environments, tasks may often involve movement in steep slopes or climbing steep walls. Robots with anthropoid features are the best candidates for performing the tasks in a hard environment [3], [4].

Anthropoid robots are increasingly important for working in remote environments, e.g., deep sea and outer space [5], [6]. Researchers at the German Research Center for Artificial Intelligence (DFKI), Robotics Innovation Center and the University of Bremen have developed "Charlie," an ape-like robot. The quadruped posture of Charlie is more stable than a bipedal posture. Therefore, the robot is well equipped to deal with the exploration of rough and bumpy

environments like lunar craters. Due to the ability of the robot to stand upright on two legs, the forelimbs can be used for handling a task and other complex humanoid motions [4], [7].

While navigating in a difficult terrain, the biological systems increase the efficiency with a robust set of strategies for locomotion [8]. However, the drivers of the bipedal humanoid walking robots are typically limited in their range of motion. Bipedal motion is only one aspect of the versatility of the hominid musculoskeletal system. Humans and apes comfortably and habitually acquire a diverse range of gaits and movement patterns in order to navigate on the ground and on the trees. The kinematic similarity between quadrupedal and bipedal gaits in hominids is reflected in the metabolic cost of these locomotor modes. The oxygen consumption measurements of the chimpanzees on a treadmill have shown that bipedal gaits and quadrupedal walking require the same amount of metabolic energy [9]. Biomechanical analysis of chimpanzees indicates that quadrupedal walking and bipedal gaits are equally expensive as they require similar amounts of muscle activation to support the chimpanzee's body weight [10]. This finding supports the choice of developing a robot that uses four legs to move on the surfaces and using the bipedal stance only when necessary. This choice also reduces the need for complex controllers for bipedal walking motions.

There has been insufficient research focusing on humanoid robots in underwater environments. Few studies have focused on the robot configurations with partially humanoid bodies, such as the Red Sea Robotic Exploratorium project [11].

B. REVIEW STAGE

Any kind of work in underwater structures, e.g., boat hulls, oil platforms, construction on ports, bridge piers, and dams, or on the seabed generally requires devices that can move and rest on the surface of the work [12]. Two classes of movement are involved in underwater work. Some underwater tasks involve navigation by propulsion, such as exploration, gathering of samples or carrying out mechanical work if the task is performed remotely on a specific place of the surface. In such cases, remotely operated underwater vehicles (ROVs) are often used [13], [14].

To manipulate objects in the oceanic environment, ROVs often carry arms with special tools. Moving a tool arm in an underwater environment is complicated due to the underwater currents and potential collisions with seabed obstacles. ROVs are generally unfit to travel along the bottom of the sea, even for a very short distance. The obstacles on the seafloor can affect the stability of navigation and possibly cause serious mechanical damage to vehicles.

The other underwater tasks are performed near or immediately above the ocean surface. In such cases, the vehicle that performs the task must move its limbs to walk, crawl, or slide on the work surface. This is a major functional constraint for the robot design. Such a robot needs extremities that can move along the surface, hold onto the seafloor, and perform

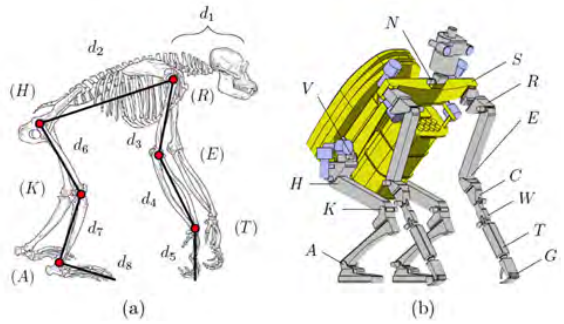

FIGURE 1. Pan troglodytes skeleton in a quadruped pose (a), and schematic view of the underwater anthropoid robot (b).

complex tasks. Anthropomorphic devices are well suited for this set of tasks.

A robot that can both propel itself through the water and walk along the seabed is well suited for performing tasks on remote parts of the ocean floor. Currently, an underwater device that can navigate like an ROV and walk on a surface like a hominid is not available.

II. CONTRIBUTION OF THIS PAPER

This article contributes to the development of robotic technologies for working near the underwater surfaces and on the seabed. The work on a hybrid 24-DoF robot is reviewed in detail, along with discussion on the modeling process, design decisions, manufacturing, and control scheme. In particular, (a) modularity of the robot design and (b) the hybrid function that transforms the robot from an ROV-like mode into a multi-articulated robot with legs for walking on irregular surfaces can be referred to as novel contributions. In experimental tests, the effectiveness of a 24-DoF hydraulic control system was demonstrated and the robot prototype was lightweight as well as manufactured and controlled easily and has maneuverability.

III. ROBOT DESIGN

The developed anthropoid robot has 24 DoF and is driven by hydraulic actuators. The robot requires an external hydraulic power source, similar to most ROVs. As shown in Fig. 1, the underwater robot is designed with geometric proportions similar to those found in Pan troglodytes (i.e., chimpanzees). Within the suborder Anthropoidea, these primates can move on four limbs in unstructured environments and often perform manual tasks that require dexterity and accuracy. Several recently developed robots use anthropoid geometry [15]–[17].

The proportions of the body segments were extracted from an anatomical study [18] to calculate the links of the underwater robot (Tables 1 and 2). The robot joints are labeled in Fig. 1, and their parameters are listed in Table 1. The length parameters "di" are normalized for an upper-arm length of 500 mm. The robot is around 1.6-m tall in its quadruped configuration and has an estimated maximum weight of 150 kg in air. Hence, the robot in the vehicle mode

TABLE 1. Robot dimensions based on Pan troglodytes proportions.

Segment	Parameter	Proportion (d = 500 mm)	Calculated value (mm)	Selected value (mm)
head	d1	0.8d	400	400
torso	d2	1.9d	950	955
upper-arm	d3	d	500	500
forearm	d4	d	500	580
hand	d5	0.8d	400	240
thigh	d6	d	500	500
calf	d7	0.7d	350	500
foot	d8	0.8d	400	500

TABLE 2. Notation for rotational joints with hydraulic actuation.

joint	DOF	parameter	joint	DOF	parameter
neck	1	N	hand	1	G
shoulder	2	S, R	hip	2	V, H
elbow	1	E	knee	1	K
wrist	3	C, W, T	ankle	1	A

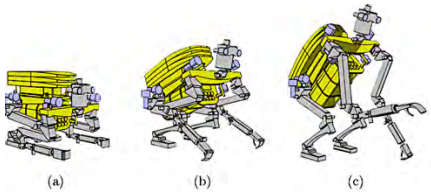

FIGURE 2. Pan troglodytes skeleton in ROV (a), quadruped pose (b), and anthropoid pose (c).

is expected to have the size and weight of a small working-class ROV, comparable with commercial underwater vehicles.

An underwater robot with an anthropoid structure is advantageous for the stability of its quadruped locomotion and versatility for climbing and grasping objects. An anthropoid body shape is well adapted for existing facilities and tools meant for human use. Furthermore it is well suited to intuitive teleoperation methods.

A. ROBOT DESIGN

As Fig. 2 depicts, the underwater robot is designed with the capability to transform between two different configurations, with an anthropoid mode and a vehicle mode. In anthropoid mode, the robot can be operated remotely by one or more pilots to perform physical interventions underwater. Since the robot and human pilot have similar kinematic structures, the robot can be controlled intuitively using an exoskeleton or motion capture system. The arms and legs can also be used to move the robot over short distances in tight spaces where the propellers may be impractical for use. The vehicle-mode configuration presents minimized drag forces, enabling efficient long-distance movement through the water. The robot can be operated remotely in this mode using a joystick or any master device, e.g., ROV. The remaining technologies have been developed for handling underwater vehicles, such as launch and recovery systems (LARS) or tether management systems (TMSs). It can be implemented directly with the present robot design.

Transitions between modes can be realized in different ways depending on the available propulsion and ballast systems. One possible transition occurs when the robot lands in the vehicle mode on the seabed or the working area, changes from positive to negative buoyancy, and stands up using its arms and legs simultaneously to reach the anthropoid configuration.

TABLE 3. Robot's technical characteristics.

No.	Component	Description
1	servovalves	Huantog. HT-803/10 (10 L/min @ 7 MPa; 40 mA)
2	hydraulic cylinders	SMC. CHNC25-200 / CHNL25-200 (7 MPa)
3	hydraulic motors	AS Hydraulic. BMM40MAIEB (9 MPa)
4	mechanical structure	Inox steel/aluminum/high-density polyetilen
5	joint sensors - encoders	ELTRAN; EMA22A2048B5SPX8S10PR3
6	electric thrusters	crust crawler; Hi-Flow 400 HFS-L thruster
7	depth sensors	KELLER; Keller PAA-21S/80549.3
8	inertial units	SparkFun; nine-DoF Razor IMU
9	on-board computer	national instrument; cRIO 9022/cRIO 9114 FPGA LX50 Virtex-5 (eight slots)
10	imaging sonar	Tritech; Micron Sonar (RS485)
11	3D camera	Diotronic; medium-speed intelligent dome PTZ

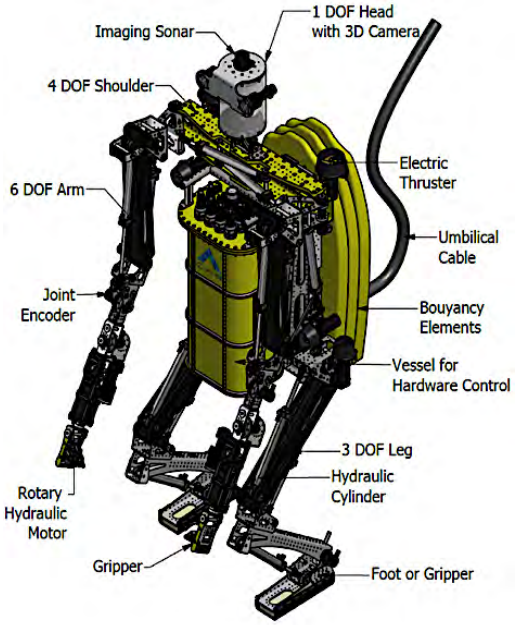

FIGURE 3. Robot's mechanical design.

B. TECHNICAL ESPECIFICATIONS

Table 3 lists the technical data, and Fig. 3 illustrates the central mechanical, hydraulic, and electrical hardware of the robot.

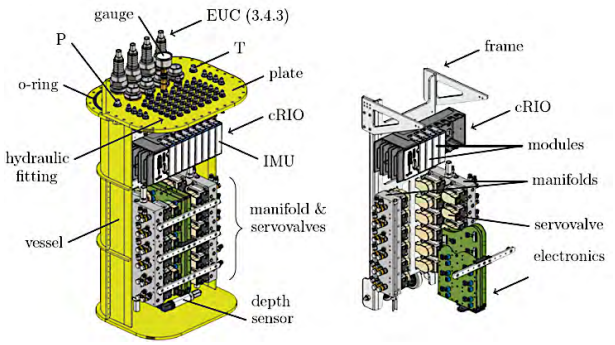

FIGURE 4. Module 1. (a) Design of the trunk with servovalves HT-803/10, rated pressure of 7 MPa, rated flow of 10 L/min, and a frequency response of 100 Hz.

C. MODULAR DEVELOPMENT

Modular design is a powerful concept in the development of a complex system. The 24-DoF robot shown in Fig. 3 can be simplified with a modular design. Four basic modules were acquired. The main module is the trunk of the robot, on which the three remaining modules are assembled. The control architecture is designed such that the hydraulic servos are housed inside the trunk according to the symmetry of each module, as are the electronic controls and the sensors. Fig. 4 illustrates the design of the robot trunk (Module 1).

The trunk was designed as a compact structure to which the arms and the legs are connected, and comprises the hardware control core. The control housing is articulated to facilitate the assembly and maintenance. The left–right symmetry of the humanoid robot was considered throughout the design. The division of the hydraulic port plates and the electrical connections was designed with consideration of the requirements of the electrical and hydraulic connections. Fig. 4 shows the two lateral plates for each side of the robot on which the servovalves are assembled. These plates also distribute power to each hydraulic servovalve. The control boards and power for the servovalves are located in the center of the plates.

Fig. 5 illustrates the design of the upper limbs. The most important structural part of this module is the shoulder. The hydraulically actuated arms are assembled in the shoulder. In addition, the hydraulic cylinders are placed over the shoulder, as shown in Fig. 5. The robot arm has six DoF (see Table 2) and is formed by two segments: the upper arm and the forearm. The robot arm is made from high-density polyethylene, aluminum, bronze, and stainless steel. The smaller parts are 3D printed on ABS plastic. The upper arm contains three rotational joints, and the shoulder joint (S) is actuated from the robot torso. The rest are actuated by two opposite inverted slider-crank mechanisms (ISC), one for the shoulder joint (R) and another for the elbow joint (E). The ISC linkages share the upper connecting link.

Fig. 6 illustrates the design of the legs. Each leg of the robot is operated by three hydraulic actuators. The mechanical structure is formed by the joints that combine the parts of plastic and stainless steel that were laser cut and folded.

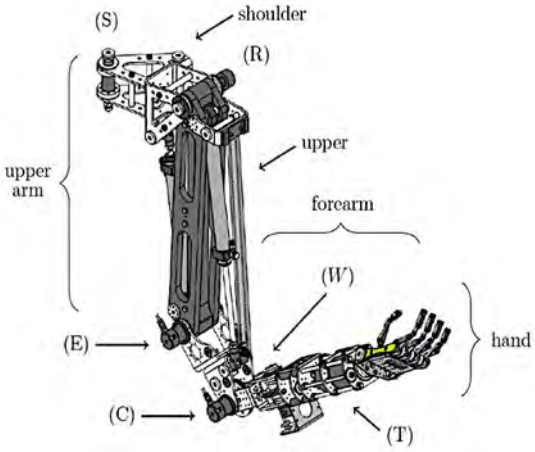

FIGURE 5. Module 2. Design of one of the hydraulic arms.

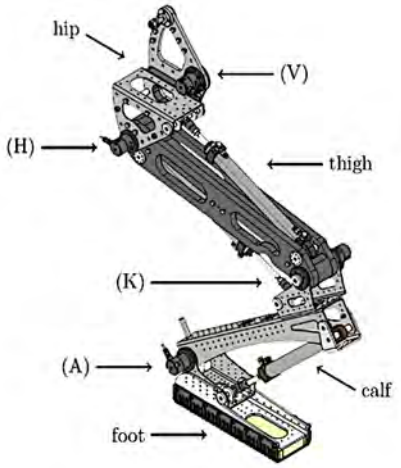

FIGURE 6. Module 3. Design of the robot leg. (V) and (H) are the hip joints, (K) is the knee joint, and (A) is the ankle joint of the robot.

The robot leg has 4 DoF (Table 2) and four links. The rear limbs are made of stainless steel, bronze, and high-density polyethylene. The small parts are manufactured from aluminum and 3D printed ABS plastic. The rotational hip joint (V) is actuated from the robot trunk. The thigh link is like the upper link of the arm; hence, the rotational hip joint (H) and knee joint (K) are moved by two opposite ISC mechanisms and share the thigh link in common. The calf link and the rotational ankle joint (A) are part of a single inverted slider-crank linkage, which orients the foot along the sagittal plane of the robot.

As Fig. 7 shows, the underwater robot is fitted with a propulsion system. It includes multiple electric thrusters that are driven by brushless motors. The thrusters are aligned with the principal axes of the robot motion in the vehicle mode. Additionally, they must be powerful enough to overcome the resistive forces exerted on the vehicle as it moves through the water.

For steady motion, the thrust and drag forces should be balanced. Therefore, the required thrust can be roughly

FIGURE 7. Module 2. Hi-Flow 400 HFS-L thruster.

TABLE 4. Notation for rotational joints with hydraulic actuation.

parameter	ρ	C_D	A^Z	DOF
value	1000 kg/m^3	2	0.8 m^2	0.5 m/s

estimated using the following equation [19]:

$$f_D^z = \frac{1}{2}\rho C_D A^Z \omega^2, \tag{1}$$

where ρ denotes the water density, C_D is a dimensionless drag coefficient, A_z is the frontal area along the $z-$axis and ω is the linear velocity along the same axis. According to Moore (2010), for a non-streamlined vehicle, C_D can take values greater than 1. For this open-frame robot, the drag coefficient is assumed to be 2 (CD $=$ 2) to ensure that the propulsion system is sufficiently powered. In the same way, the z-axis has been chosen for thrust calculations because the vehicle presents the maximum frontal area along that direction.

Equation (1) is solved for the parameters listed in Table 4, which yields

$$f_D^z = 200N. \tag{2}$$

Thrusters are generally designed to provide their maximum thrust in a fixed position. As the vehicle moves under the water, the forward speed of the thrust decreases around 10% per knot [20]. Subsequently, the thrust required when the robot moves at 0.5 m/s (≈0.972 kn) is calculated as follows:

$$f_T = \frac{f_D^z}{0.9^{(0.972)}} = 221.6N. \tag{3}$$

At a relatively low cost, compared to similar models, the Hi-Flow 400 HFS-L thruster provides maximum thrust of 67 N, as shown in Fig. 7. Therefore, eight thrusters are used to propel the underwater vehicle with 3 DoF. Four electric thrusters of this type are installed in parallel to the z-axis for depth positioning. Another four thrusters are placed in parallel to the x-axis to control the heading and forward speeds.

IV. ONBOARD CONTROL SYSTEM

Fig. 8 shows the control block diagram of the robot's ROV-mode navigation system. Note that e_q and e_p are the attitude and position errors, respectively; u is the control law; f_T is the driven torque of the thrusters; and η is the path vector.

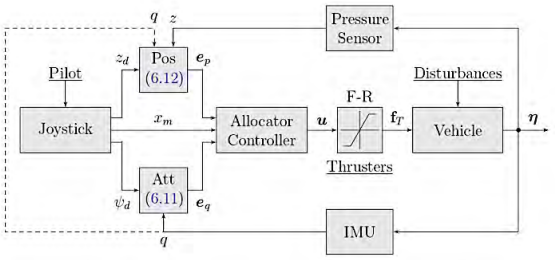

FIGURE 8. Block diagram of the navigation control.

TABLE 5. Notation for rotational joints with hydraulic actuation.

Layer.	Name	Description
1	JOINT	state configuration of the servohydraulic actuators
2	PID	PID controllers configuration for walking
3	WALKING	humanoid walking configuration
4	AUX	auxiliary control variable configuration
5	THRUSTER	PID controllers configuration for navigation
6	AUTOPILOTS	mission configuration for ROV navigation
7	MASTER	external control devices' (joysticks, MasterSuit) configuration
8	DATA	experimental data register configuration

The control system and interface of the experimental robot were developed to be used use as a second computer on the board of robot, as shown in Fig. 4. The National Instruments cRIO 9022/9114 cRIO Virtex-5 LX50 field-programmable gate array (FPGA; eight slots) was programmed with LabVIEW for this purpose. The control system and the experimental interface are based on eight-layer systems, which are summarized in Table 5.

In the "MASTER" layer, the communications are configured with devices for external control. The external device can be a MasterSuit, a joystick, or mission control operating through the "WALKING" or "AUTOPILOT" layers. In the "MASTER" layer, the communication with the haptic teleoperation suit is enabled by pressing the "External Input Mode" button. By pressing the "EI-MODE"/"ENABLE PS3 JOYSTICK" button, the communications with commands from the "WALKING" or "AUTOPILOT" layers are enabled.

A. TRANSFORMER'S EXPERIMENTAL TESTS AND RESULTS

This section presents the practical results that have been achieved throughout the development of the robot. The robot transformation process from ROV to humanoid configuration can be performed in a marine-free space, as shown in Fig. 10. However, it is not practical because placing the robot on the seabed after its transformation into a humanoid is challenging. The transformation experiments have been performed after the robot has landed on the seabed, following the sequence shown in Fig. 2.

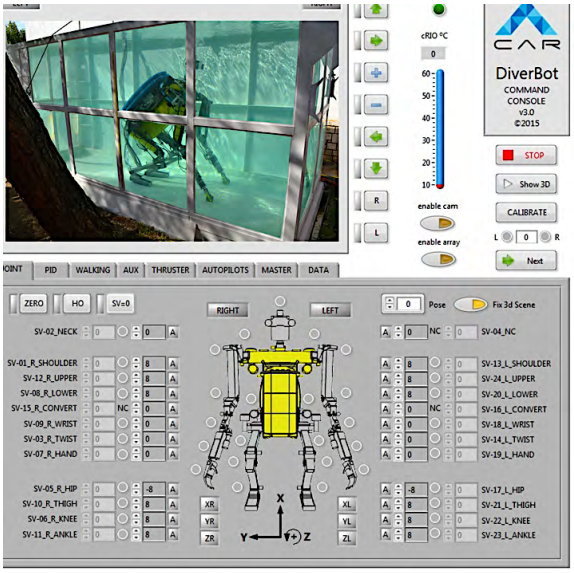

FIGURE 9. Screenshot of MasterBot multilayer control. The joint-control interface is shown.

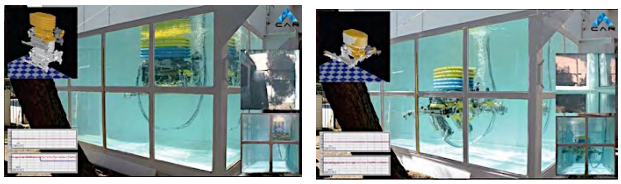

FIGURE 10. Navigation and example of transformation from ROV to humanoid in the marine-free space.

As demonstrated in a previous study [32], a classical PI controller could be used for position control [29]. Despite the presence of a hydraulic servo actuator (HPA), the model presents a pole at the origin. A simple P controller does not eliminate the steady-state error since input step disturbances occur before the integrator, producing a ramp disturbance, which cannot be rejected by this controller. Conversely, PD and PID controllers produce noisy outputs, which are not suitable for position control [33]. To cancel the steady error, a linear PI controller is implemented for each robot joint (Fig. 11). The constant integrator time should be carefully adjusted because the PI controller adds another integrator to the closed-loop system and thus reduces the system stability.

Although the transformation process of the robot can be controlled via several strategies, decentralized PI control is implemented herein. The concept of decentralized control has been adopted due to the use of the hydraulic robot power system, which is robust against perturbations. Thus, the PI controller is sufficient for validating the kinetic algorithms for the change of the condition from ROV to humanoid.

Fig. 12 shows the results of the leg (Fig. 6) movement of the robot. The step is applied on the hip joint from the configuration shown in Fig. 13(a). Fig. 13(b) shows that before 26°, the average response time is 8 s.

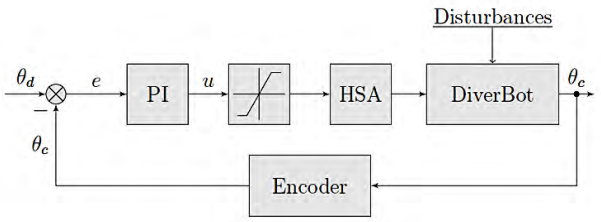

FIGURE 11. PI Control scheme for servo-position loop.

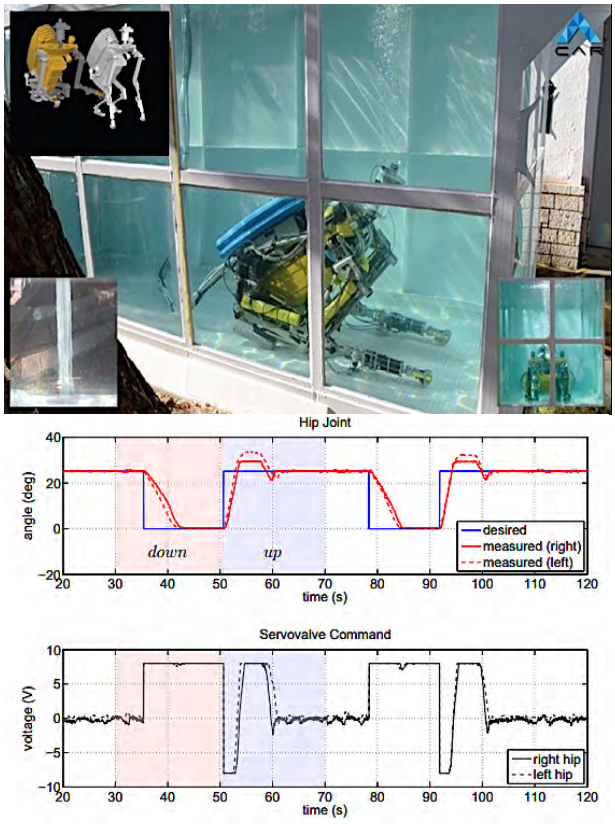

FIGURE 12. Navigation and transformer's practical results.

B. WALKING EXPERIMENTAL TESTS AND RESULTS

The walking process of an anthropoid robot on the seabed is enormously complex. Therefore, several factors must be considered. Robots with buoyancy close to zero must contact the seabed as they would be in a low-gravity environment.

Under these circumstances, the friction between the robot feet and the floor surface is only possible if the marine thrusters supply a downward force. As shown in Fig. 14(a), in the first phase of robot development, the robot was tested for walking on a flat surface to test the balancing algorithm.

When the underwater robot is in the humanoid mode, it can move on the seabed by walking on both forelimbs and rear limbs. Several ape-like walking robots have been developed in the past decades [15], [16] due to the advantages of legged robots over wheeled and tracked systems for locomotion in complex terrain.

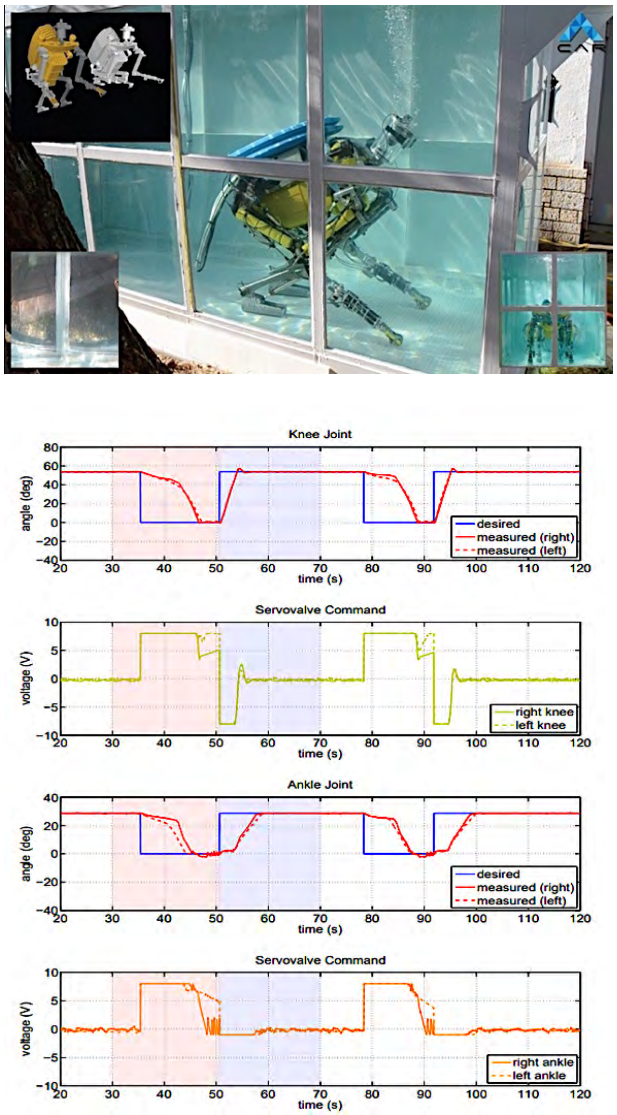

FIGURE 13. Navigation and transformer's practical results.

In some cases, underwater locomotion is easier than terrestrial motion. For low-speed motions, buoyant forces are dominant over hydrodynamic forces, reducing the effective weight of the robot in water. In this case, the kinematics of the robot can be calculated and verified using a terrestrial locomotion with reduced gravity [21], [29].

Fig. 14(a) depicts the calculation process for performing statically stable walking at low speeds, assuming well-defined trajectories in Cartesian space according to the surface of the seabed. For example, in horizontal and flat terrain, the robot can follow a cycloidal path that produces continuous and smooth joint trajectories in space. The forelimbs and rear limbs of the robot can be analyzed as planar 3R manipulators. With this model, the inverse kinematics can be solved analytically with a closed-form solution [22], [23].

During the stride phase, the robot moves one of the limbs through a cycloidal Cartesian trajectory (Fig. 14(a)). The stance phase is calculated as a closed kinematic chain, following a cycloidal curve at the level of the hips [22]. Once the joint trajectories are calculated, they are used together with the robot mass parameters to compute the instantaneous center of gravity (CG) of the robot. This calculation follows the statically equivalent serial chain method (SESC) [6]. During low-speed locomotion, the CG position can be represented with the end-point position of the equivalent open serial kinematic chain. The geometric parameters depend on the mass properties of the original structure. In the underwater case, effective weight in the water and the position of each CG link constitute the mass parameters.

At the planning level, the CG position is used to analyze the robot's static stability. The vertical projection of the CG must be included inside the support polygon that contains all the contact points between the robot and the ground [24].

Fig. 14(b) shows some experimental results. The curves show the time evolution of the robot trunk orientation during quadrupedal locomotion. Pitch and roll angles are $\sim 0°$, indicating stable motion. This indicates that the planned cycloidal walking path is accurate. Additionally, the kinematics coordination of the trunk and arms enable a smooth displacement of the anthropoid robot, with its trunk inclined in 45° in quadruped motion.

V. RESULTS AND DISCUSSION

A. ROBOT KINEMATICS

When exploring difficult access terrains, the biological systems appear to be more efficient as them employ quadrupedal strategies for locomotion. In the case of chimpanzees and other hominids, the quadrupedal knuckle-walking locomotion is frequently used for displacements in terrestrial and tree-like environments.

The kinematic similarity between the quadrupedal and bipedal gaits is reflected in the metabolic cost of these locomotor modes. Studies based on treadmill oxygen consumption measurements of chimpanzees have shown that bipedal and knuckle-walking locomotion require the same amount of metabolic energy.

Similarly, in comparison with bipedal robots, quadrupedal robots generally better adapted to locomotion in rugged terrains or wheeled and tracked systems. Among the most advanced quadrupedal robots, the BigDog robot is prepared for dynamic locomotion under extreme conditions [34] Moreover, Charlie is designed for research on multi-locomotion modes for spatial applications [35]. However, neither of these prototypes are designed for underwater operation. The surface of the seabed tends to be irregular, which make the legs advantageous for locomotion [30]. In an underwater environment, the robot can also use marine propulsion to avoid obstacles. Kinematics calculations of the bipedal configuration allow the robot to use its forelimbs for executing its tasks. It is necessary to use the impellers to press the robot onto the seafloor because of the null buoyancy of the robot.

Due to the similarity between the kinematics of the robot and the human operator, the robot can be controlled with gestural signals [25]. Human gestures convey a large

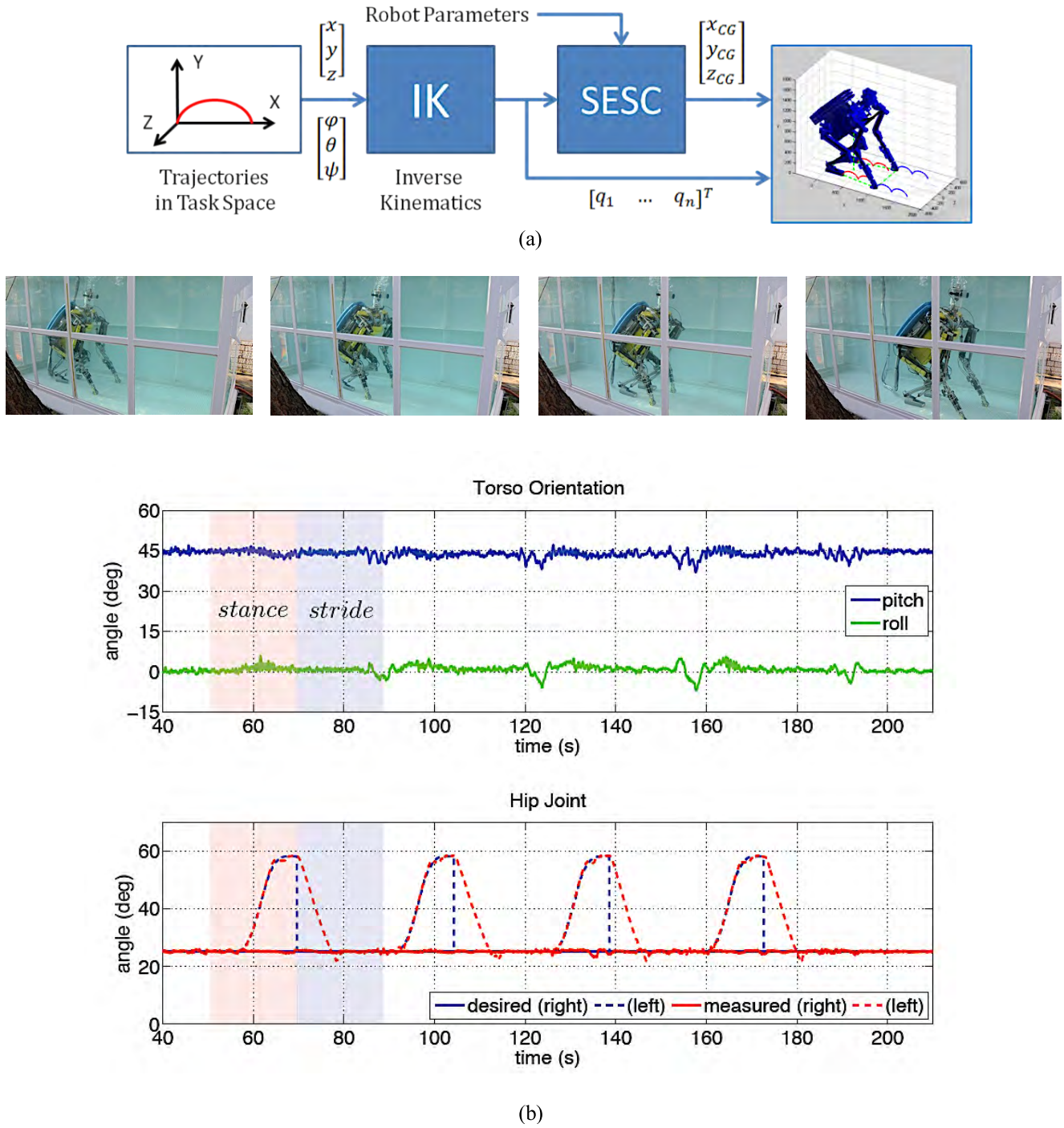

FIGURE 14. Practical results for the walking case.

quantity of information. Motion tracking and gesture recognition are essential for developing novel devices capable of naturally and synergistically interacting with the human operators [25]–[27]. Fig. 16 shows SmartSuit—the wearable master/slave interface [28]. SmartSuit is a bidirectional device; it can send a command to a remote device and receive information from the remote device.

B. ACTUATORS AND POWER SYSTEM

There are two options for the actuation systems of a hybrid robot, electric drives or hydraulic drives. Electric motors are not suited to the task. They must be special-purpose motors and sealed. Furthermore, they require a huge amount of electrical cables for power and sensors. The electronics power must be watertight, bulky, and heavy. It also increases the

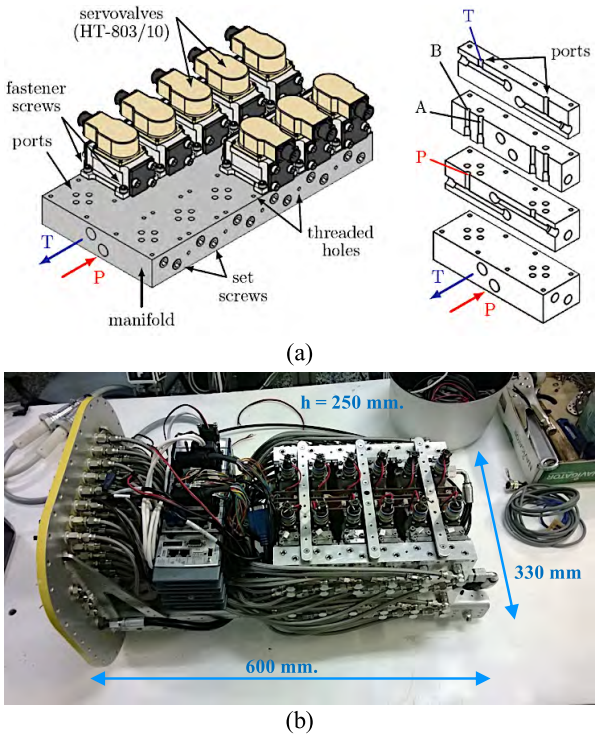

FIGURE 15. **(a) Hydraulic circuit for 24-DoF servovalves and (b) control vessel.**

complexity and the size of the robot. On the other hand, hydraulic actuators are compact and lightweight. Servovalves can be grouped in an ultracompact manner. Fig. 15 shows the 24 servovalves that are packed into the trunk module, along with the electronic amplifiers for the servovalves and the on-board cRIO computer. This compaction is possible because of the custom valve plates, each of which has capacity for 12 valves, as shown in Figs. 4 and 15.

Therefore, hydraulic actuation has clear advantages for the seabed robot over an electric actuation system [29]. As mentioned before, the robot can be made extremely compact due to the weight:power ratio of the hydraulic drives. Hydraulic power can be supplied by a device on the robot or through an umbilical cord from a submarine garage. In the case of the seabed robot prototype, the hydraulic plant has been adjusted to supply 70 bar and 11 lpm.

The power module in Fig. 15 concentrates 24 servovalves with a real working capacity of 10.0 lpm and 70 Bar, which concentrates 28 KW of real power in a trunk volume of $600 \times 330 \times 250$ mm^3.

The hydraulic performance of a seabed robot is inherently watertight because of the pressure compensators. Underwater pressure compensators allow the underwater robots to work at any depth [30]. The electronic enclosures are simply filled with oil. From the standpoint of the construction of the robot, this is an excellent solution, which greatly simplifies the design, weight, and manufacturing of a multi-articulated robot.

These design features ensure that the underwater hydraulic system is watertight and can operate at any depth.

C. CONTROL SYSTEM

The onboard control of the seabed robot could use the Robot Operating System (ROS) in conjunction with a generic system or could use LabVIEW with proprietary hardware, e.g., CompactRIO (cRIO) of National Instruments (NI). In the proposed robot's development, as shown in Fig. 13, the NI cRIO hardware was chosen considering the cRIO's dimensions, number of modules, and available memory for the FPGA.

cRIO controller is used to manage the sensors and actuators of the underwater robot. cRIO is a reconfigurable embedded system made by NI for industrial control applications. It includes a processor running a real-time operating system (RTOS), a reconfigurable FPGA, and interchangeable I/O modules (Fig. 3.15).

The cRIO-9022 controller features an industrial 533-MHz Freescale MPC8347 real-time processor and contains 256 MB of DDR2 RAM and 2 GB of nonvolatile storage for storing programs (NI, 2014). The controller provides two Ethernet ports for network communication and connects to cRIO-9114 reconfigurable eight-slot chassis, fitted with a Virtex-5 LX50 FPGA developed by Xilinx.

The I/O modules allow us to connect sensors and actuators to the embedded controller. The module NI 9871 has four ports for serial data communication, one of which is used to send commands to the PTZ dome camera, while the other is used to read the orientation data provided by the IMU. Two digital I/O modules (NI 9403) are used to receive the encoder position. Another digital I/O module (NI 9201) is used to send PWM control signals to the electric thrusters.

Two analog output modules (NI 9264) are used to output a voltage signal to the flow control servovalves. An analog input module (NI 9201) is used for the pressure sensor readings. A slot filler module (NI 9977) is employed to house a nine-DOF Razor IMU with a fixed orientation inside the control unit (see Table 3).

The robot joints are measured by absolute magnetic encoders Eltra EMA22$*$, with 2048 pulses per revolution of resolution and synchronous serial interface (SSI) output. The SSI interface transmits the absolute encoder position via a serial data line synchronized by a clock signal. The SSI signals are transmitted differentially (RS422) to avoid interferences in longer transmission distances.

The master interface is formed by an RS422 transceiver MAX3087†, which is used to generate differential signals from/to digital I/O ports. MAX3087 is a high-speed transceiver for RS485/RS422 communication. It contains one driver and one receiver (full-duplex communication).

The coils of servovalve HT-803/10 are connected in parallel and can be commanded by a $\pm$40-mA current signal. The first circuit stage is formed by a voltage buffer using an operational amplifier (OPA552). Another OPA552 is used to convert the $\pm$10-V voltage signal of the cRIO module (NI 9264) into a current signal of $\pm$40 mA for the servovalve.

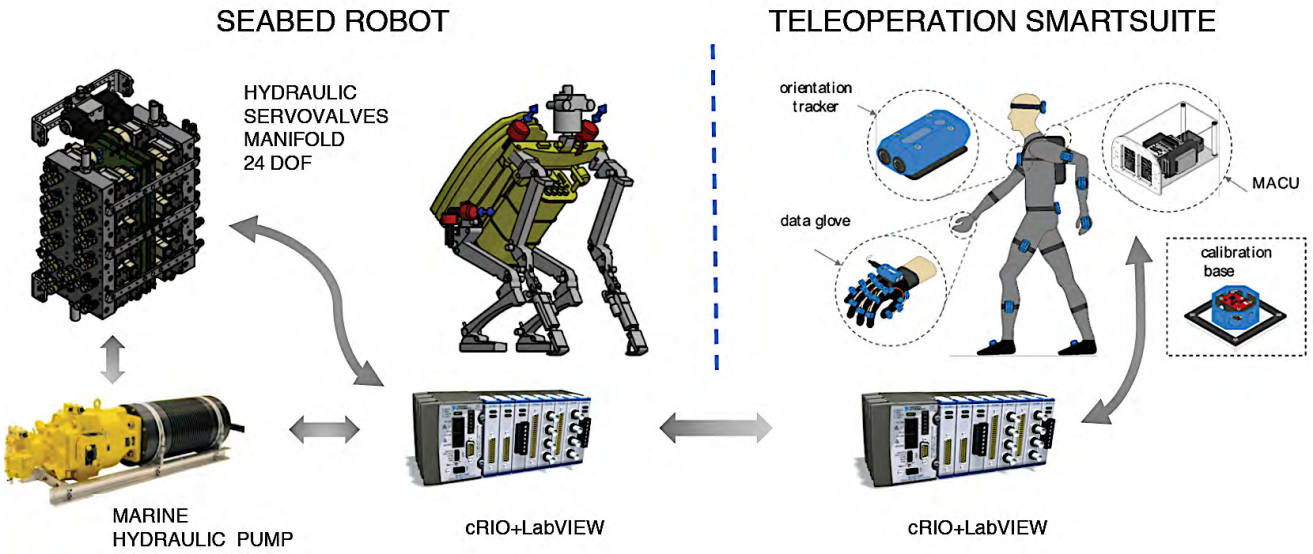

FIGURE 16. Design of the 24 DoF control system for seabed work controlled remotely by an operator using gestures and implemented in real-time hardware using the cRIO computer.

Such op amps have high current capability (200 mA), which is suitable for servo applications‡.

The real-time controller provides a uniform update rate, which is interesting for the implementation of control algorithms. Considering that the robot is designed for low-speed motion in a high-density environment, the system bandwidth is assumed to be relatively low. To realize accurate control, the controller frequency must be higher than the system bandwidth; thus, an update rate of at least 50 ms is adopted for this application.

The cRIO hardware and its modules are precisely adapted to the requirements of the space of the mechanical design of the torso module. The development times for the control architecture were minimized by adopting a development specification based on cascading software development. This approach is consistent with the control of the robot by means of a teleoperation avatar, which is based on a high-level gestural language. It is combined with the on-board implementations of algorithms that control robot's walking and navigation activities. Fig. 16 illustrates the loop control for each joint, which is implanted in the FPGA memory of cRIO.

VI. CONCLUSIONS

This article presents initial practical tests of a robot for seabed operations and introduces a design for a teleoperation scheme. This scheme allows an operator to articulate the robot with full-body gestural commands. In experiments with marine navigation, walking and manipulation of the robot are controlled by gestures. The development of seabed robots with the morphologies of humanoid kinematics was experimentally demonstrated herein and their CAR UPM-CSIC researchers in several studies [28]–[33].

These tests confirm that the hydraulic power systems for humanoid seabed robots solve the problem of water tightness with the aid of hydraulic technology, which it is inherently sealed. The only component of the robot that needs to be tight is the trunk (see Fig. 4). To seal this component, the trunk is filled with mineral oil and a pressure-compensating device is installed [30]. The pressure compensator automatically balances the external pressure from the inside of the tank. From the mechanical design standpoint, the weight and manufacturing complexity involved when dealing with multiple DOFs pose a problem. Therefore, hydraulics technology offers the best solution.

Finally, the control system based on a specific apparatus, e.g., cRIO, allows us to create an ultracompact design for multiple DOFs and enables rapid control software development in real-time architecture with the aid of the LabVIEW language. If it is necessary to implement ROS in future development of this robot, the LabVIEW package and ROS can be easily integrated.

ACKNOWLEDGMENT

The authors are grateful for the valuable collaboration with Dr. Gonzalo Ejarque and Mr. Gabriel Poletti of the Group of Robots and Intelligent Machines of the Center for Automation and Robotics. Furthermore, they appreciate their participation in the diver BOT-DPI2009-08778 project, under which they conducted their PhD studies.

REFERENCES

[1] F. Zhang, G. Marani, R. N. Smith, and H. T. Choi, "Future trends in marine robotics [TC spotlight]," *IEEE Robot. Autom. Mag.*, vol. 22, no. 1, pp. 14–122, Mar. 2015.

[2] S. Y. Shin and C. Kim, "Human-like motion generation and control for humanoid's dual arm object manipulation," *IEEE Trans. Ind. Eng.*, vol. 62, no. 4, pp. 2265–2276, Apr. 2015.

[3] T. Kaneko and M. Tomonaga, "Differential reliance of chimpanzees and humans on automatic and deliberate control of motor actions," *Cognition*, vol. 131, no. 3, pp. 355–366, Jun. 2014.

[4] H. Pontzer, D. A. Raichlen, and P. S. Rodman, "Bipedal and quadrupedal locomotion in chimpanzees," *J. Hum. Evol.*, vol. 66, pp. 64–82, Jan. 2014.

[5] H. Karaś, "Robotics in mining," in *Proc. EUMICON Design Future*. Linz, Austria: voestalpine Stahlwelt, May 2015.

[6] S.-M. Yoon *et al.*, "Track velocity control of crawler type underwater mining robot through shallow-water test," *J. Mech. Sci. Technol.*, vol. 26, no. 10, pp. 3291–3298, 2012. [Online]. Available: www.springerlink.com/content/1738-494x, doi: 10.1007/s12206-L012-0810-2.

[7] *iStruct Intelligent Structures for Mobile Robots*. [Online]. Available: http://robotik.dfki-bremen.de/en/research/projects/istruct-1.html

[8] A. Stentz *et al.*, "CHIMP, the CMU highly intelligent mobile platform," *J. Field Robot.*, vol. 32, no. 2, pp. 209–228, 2015.

[9] C. R. Taylor and V. J. Rowntree, "Running on two or on four legs: Which consumes more energy?" *Science*, vol. 179, no. 4069, pp. 186–187, 1973.

[10] M. D. Sockol, D. A. Raichlen, and H. Pontzer, "Chimpanzee locomotor energetics and the origin of human bipedalism," *Proc. Nat. Acad. Sci. USA*, vol. 104, no. 30, pp. 12265–12269, 2007.

[11] *The Red Sea Robotic ExploratORIUM*. [Online]. Available: http://cs.stanford.edu/group/manips/projects/redsearobotics.html

[12] E. Cole, "Mining the seafloor with robots," *Robot. Trends*, Feb. 2012.

[13] R. Bogue, "Underwater robots: A review of technologies and applications," *Ind. Robot, Int. J.*, vol. 42, no. 3, pp. 186–191, 2015.

[14] G. L. Antonelli, *Underwater Robots: Motion and Force Control of Vehicle-Manipulator Systems*. Berlin, Germany: Springer, 2006.

[15] W. Weiguo, W. Yu, L. Feng, and R. Bingyin, "Development of modular combinational gorilla robot system," in *Proc. IEEE Int. Conf. Robot. Biomimetics (ROBIO)*, Aug. 2004, pp. 437–440.

[16] D. Kühn, M. Römmermann, N. Sauthoff, F. Grimminger, and F. Kirchner, "Concept evaluation of a new biologically inspired robot 'LittleApe,'" in *Proc. IEEE/RSJ Int. Conf. Intell. Robots Syst. (IROS)*, Oct. 2009, pp. 589–594.

[17] K. Fondahl *et al.*, "An adaptive sensor foot for a bipedal and quadrupedal robot," in *Proc. 4th IEEE RAS & EMBS Int. Conf. Biomed. Robot. Biomech. (BioRob)*, Jun. 2012, pp. 270–275.

[18] K. Schoonaert, K. D'Août, and P. Aerts, "Morphometrics and inertial properties in the body segments of chimpanzees *(Pan troglodytes)*," *J. Anatomy*, vol. 210, no. 5, pp. 518–531, 2007.

[19] T. I. Fossen, *Marine Control Systems Guidance, Navigation, and Control of Ships, Rigs and Underwater Vehicles*, Trondheim, Norway: Marine Cybernetics, 2002.

[20] Tecnadyne, Inc. (Apr. 2012). *What Size Thrusters do i Need for my ROV or AUV [Technical Note]*. [Online]. Available: https://tecnadyne.wordpress.com/2012/04/28/what-size-thrusters-do-i-..2

[21] M. M. Martinez, R. J. Full, and M. A. Koehl, "Underwater punting by an intertidal crab: A novel gait revealed by the kinematics of pedestrian locomotion in air versus water," *J. Exp. Biol.*, vol. 201, no. 18, pp. 2609–2623, 1998.

[22] M. F. Silva, J. T. Machado, and I. S. Jesus, "Modelling and simulation of walking robots with 3 DOF legs," in *Proc. 25th IASTED Int. Conf. Modelling, Identificat. Control (MIC)*, Feb. 2006, pp. 271–276.

[23] J. J. Craig, *Introduction to Robotics: Mechanics and Control*, vol. 3. Upper Saddle River, NJ, USA: Prentice-Hall, 2005.

[24] R. B. McGhee and A. A. Frank, "On the stability properties of quadruped creeping gaits," *Math. Biosci.*, vol. 3, pp. 331–351, Aug. 1968.

[25] J.-J. Cabibihan, W.-C. So, and S. Pramanik, "Human-recognizable robotic gestures," *IEEE Trans. Auton. Mental Develop.*, vol. 4, no. 4, pp. 305–314, Dec. 2012.

[26] S. Ikemoto, H. Ben Amor, T. Minato, B. Jung, and H. Ishiguro, "Physical human-robot interaction: Mutual learning and adaptation," *IEEE Robot. Autom. Mag.*, vol. 19, no. 4, pp. 24–35, Dec. 2012.

[27] T. P. Spexard, M. Hanheide, and G. Sagerer, "Human-oriented interaction with an anthropomorphic robot," *IEEE Trans. Robot.*, vol. 23, no. 5, pp. 852–862, Oct. 2007.

[28] G. Poletti and R. Saltaren, "Sistema vestible para interacción con entornos remotos mediante información gestual y sensaciones táctiles," Spanish Patent 1 162 933U, Aug. 17, 2016.

[29] G. Ejarque, "Design and control of a transformable anthropoid robot for underwater works," Ph.D. dissertation, Dept. Autom., Ingeniería Eléct. Electrón. Inf. Ind., Univ. Politécnica de Madrid, Madrid, Spain, 2016.

[30] F. Wang and Y. Chen, "Design and experimental study of oil-based pressure-compensated underwater hydraulic system," *Proc. Inst. Mech. Eng. I, J. Syst. Control Eng.*, vol. 228, no. 4, pp. 221–232, Dec. 2013.

[31] G. Ejarque and R. Saltaren, "Robot submarino humanoide transformable," Spanish Patent 2 544 007 (A1), Aug. 26, 2015.

[32] L. J. Puglisi, "Advanced control strategies for a 6 DoF hydraulic parallel robot based on the dynamic model," Ph.D. dissertation, Univ. Politecnica de Madrid, Madrid, Spain, 2016.

[33] L. J. Puglisi, R. J. Saltaren, C. Garcia, and I. A. Banfield, "Robustness analysis of a PI controller for a hydraulic actuator," *Control Eng. Pract.*, vol. 43, pp. 94–108, Oct. 2015.

[34] F. Kirchner and D. Kühn. iStruct: Intelligent Structures for Mobile Robots. German Research Center for Artificial Intelligence (DFKI GmbH) and University of Bremen. Accessed: Aug. 2013. [Online]. Available: http://robotik.dfki-bremen.de/en/research/projects/istruct-1.html

[35] D. Wooden, M. Malchano, K. Blankespoor, A. Howardy, A. A. Rizzi, and M. Raibert, "Autonomous navigation for BigDog," in *Proc. ICRA*, Anchorage, AK, USA, 2010, pp. 4736–4741.

ROQUE SALTAREN received the bachelor's degree in mechanical engineering from the Universidad del Valle, Cali, Colombia, in 1980, in part by the M.Sc. degree in electrical engineering from the Universidad de los Andes, Bogotá, Colombia, in 1990, and the Ph.D. degree in industrial engineering from the Universidad Politécnica de Madrid, Madrid, Spain, in 1996. He is currently an Associate Professor and a Research Scientist Coordinator with the Group of Robots and Intelligent Machines, Center for Automation and Robotics UPM-CSIC.

ALEJANDRO RODRÍGUEZ BARROSO received the B.Sc. degree in industrial engineering from the Universidad Politécnica de Madrid, Spain. He is currently pursuing the Ph.D. degree with the Robotic and Intelligent Machines Research Group, Center for Automation and Robotics UPM-CSIC. His research interests include cable-driven parallel robotics, fluid power systems, and underwater robotics.

OZ YAKRANGI received the bachelor's degree in electrical engineering from Ariel University, Israel, in 2013, and the M.Sc. degree in energy engineering from the Universitat Politècnica de Catalunya, Barcelona, Spain, in 2017. He is currently pursuing the Ph.D. degree with the Robotics and Intelligent Machines Research Group, Center for Automation and Robotics UPM-CSIC, Escuela Técnica superior de Ingenieros Industriales, Universidad Politécnica de Madrid, Madrid, Spain. He is also a Researcher with the Universidad Politécnica de Madrid.